Understanding focus effects in submicron optical lithography

Chris A. Mack
National Security Agency
Fort Meade, MD 20755

In the age of submicron optical lithography, focus has become a critical process parameter. Each decrease in minimum feature size is accompanied by a corresponding decrease in depth-of-focus (DOF). Sources of focus errors, such as wafer warpage, topography, and the thickness of the photoresist, however, are not being reduced in proportion to the DOF. Thus, the effects of focus on the practical resolution capabilities of a lithographic tool are becoming increasingly important.

In describing the resolution and depth-of-focus of a lithographic system, it is common to apply the Rayleigh criteria. The Rayleigh criterion for the minimum resolvable feature size is

$$Resolution = k_1 \frac{\lambda}{NA} \qquad (1)$$

where λ is the exposure wavelength, NA is the numerical aperture of the objective lens, and k_1 is a process dependent constant. Typically, k_1 is in the range of 0.4 to 0.9. Similarly, the Rayleigh depth-of-focus is given by

$$DOF = \pm k_2 \frac{\lambda}{NA^2} \qquad (2)$$

where k_2 is another process dependent constant. Values of k_2 typically are quoted in the range of 0.5 to 1.0.

In the submicron regime, the simple Rayleigh criteria are no longer adequate for describing the resolution and depth-of-focus of a microlithographic process. In this paper, alternate definitions of resolution and DOF will be given based on an understanding of the interactions of the aerial image with the photoresist process. Earlier studies [1,2] have shown that the photoresist responds to the slope of the logarithm of the aerial image. Thus, this quantity will be used as a metric for aerial image quality. The effect of defocus is to decrease the slope of the log-image. A plot of log-image slope versus defocus can be used to define both resolution and DOF simultaneously (in fact, it is impossible to define them independently). The effects of numerical aperture, wavelength, feature size, and feature type can all be characterized using this technique. Also, objective comparisons of different lithographic tools can be made.

Current lithography simulation programs predict an aerial image based on the parameters of the projection tool. This image is then used to "expose" the photoresist. A tacit assumption of these models is that the photoresist thickness is less than the depth-of-focus so that the aerial image does not change through the thickness of the resist. For the case of submicron imaging, however, this assumption is no longer adequate. The second part of this paper describes PROLITH v1.4, an enhanced version of PROLITH [3,4] which includes the effects of defocus through the resist. Using this model, the effects of exposure and focus on linewidth control and sidewall angle can be determined and asymmetric focus-exposure diagrams constructed. Also, the optimum position of the focal plane can be determined.

1. Aerial Image

In order to simplify the analysis of a lithographic process, it is highly desirable to separate the effects of the lithographic tool from the photoresist process. This can be done with reasonable accuracy only if the interaction of the tool (i.e., the aerial image) with the photoresist is known. A previous study [1] has characterized the effects of the aerial image on the photoresist with the following general results. An aerial image $I(x)$ exposes the photoresist to produce some chemical distribution $m(x)$ within the resist. This distribution is called the latent image. Many important properties of the lithographic process, such as exposure and development latitude, are a function of the gradient of the latent image $\partial m/\partial x$. Larger gradients result in improved process latitude. It has been shown that the latent image gradient is related to the aerial image by [1]

$$\frac{\partial m}{\partial x} \propto \frac{\partial lnI}{\partial x} .$$

(3)

It is important to note that the slope of the latent image is not proportional to the slope of the aerial image, but rather to the slope of the logarithm of the aerial image (the log-slope).

A second important lithographic parameter is the sidewall angle of the resist profile. There are two ways in which the aerial image affects sidewall angle. First, the latent image has a "sidewall" slope due to absorption. This slope is again directly proportional to the log-slope of the image [1]. Secondly, the very nature of the development rate process gives rise to a sloped sidewall since the top of the resist is under attack by the developer for a longer period of time than the bottom. Neglecting absorption, the slope is approximately given by [1]

$$resist \ slope \ \approx \ \frac{r(0)}{r(x)}$$

(4)

where $r(0)$ is the development rate in the center of a space and $r(x)$ is the development rate at the line-edge (i.e., at the edge of the photoresist profile). This ratio of development rates should be maximized in order to maximize the resist slope. Further, this ratio is a function of the aerial image. The simplest of approximations gives [2]

$$\frac{r(0)}{r(x)} = f\left(\frac{I(0)}{I(x)} \right) \simeq \left[\frac{I(0)}{I(x)} \right]^\gamma$$

(5)

where γ is the photoresist contrast.

The above discussion gives two ways in which the aerial image and photoresist process interact. First, the slope of the log-image affects process latitude and sidewall angle. Second, the ratio $I(0)/I(x)$ also affects sidewall angle. Thus, there are two logical metrics by which to judge the quality of the aerial image:

$$\frac{\partial lnI}{\partial x} \quad and \quad \frac{I(center)}{I(edge)} .$$

(6)

As will be shown later, the log-image slope is the preferred metric of aerial image quality. This metric has been discussed previously in relation to focus effects in the excellent work of Levinson and Arnold [5,6].

The most common metric of image quality is the image contrast, which is defined for a periodic pattern as

$$Contrast = \frac{I(center\,of\,space) - I(center\,of\,line)}{I(center\,of\,space) + I(center\,of\,line)} \quad . \tag{7}$$

The most obvious limitation of the image contrast is that it applies only to periodic patterns (and is only useful for equal lines and spaces). Also, this definition is not directly related to the lithographic parameters of interest such as latitude and sidewall angle. For these reasons, image contrast is not the best metric by which to judge the effects of defocus.
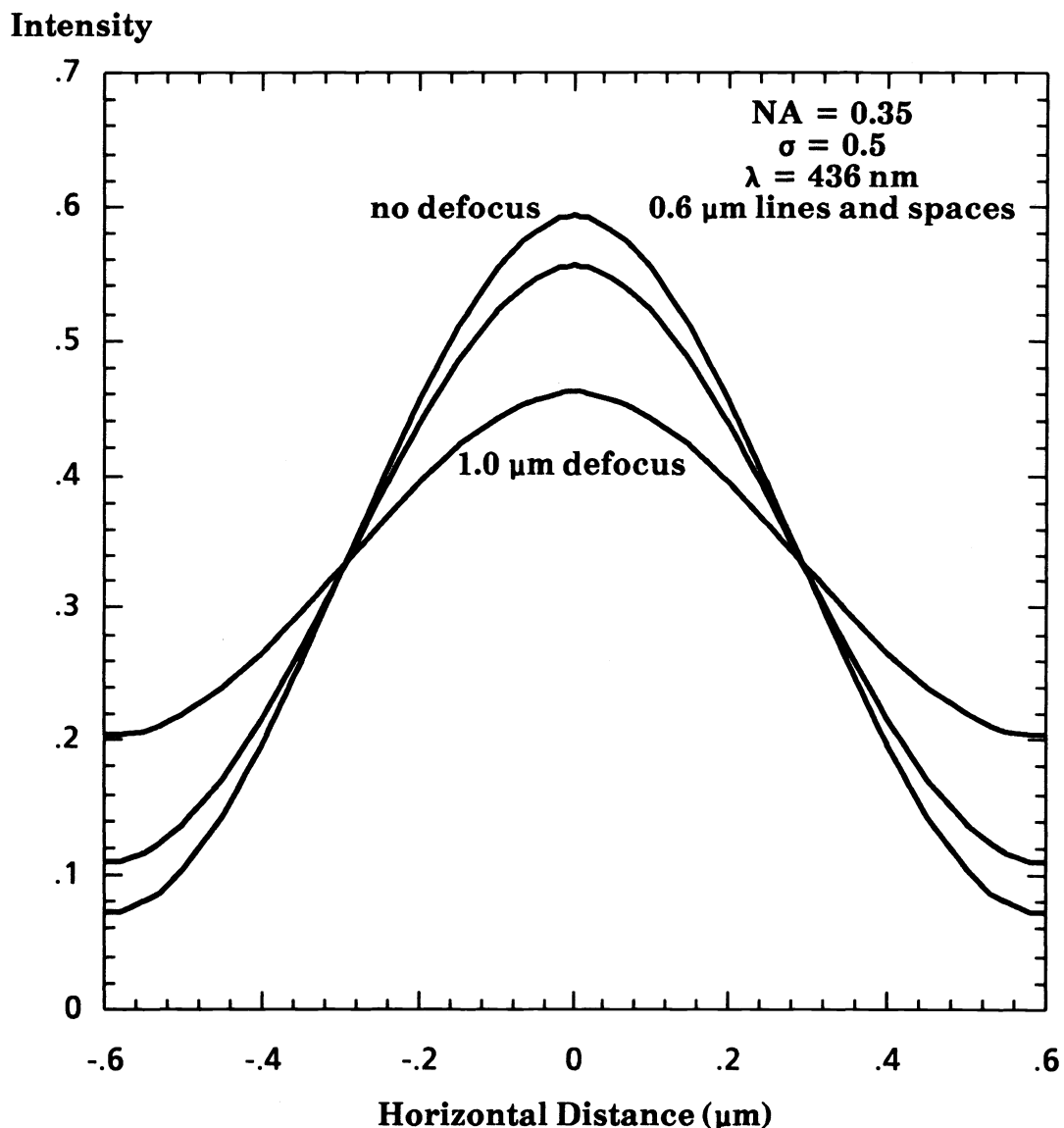

Figure 1 : The effect of defocus on the aerial image: 0, 0.5 μm, and 1.0 μm defocused aerial images were predicted using PROLITH.

2. Focus and the Aerial Image

Shown in Figure 1 is the well known effect of defocus on the aerial image. Both the edge slope of the image and the center intensity decrease with defocus. In order to examine the behavior of the log-slope, the aerial images of Figure 1 have been used to calculate the log-slope and plotted again in Figure 2. Clearly, the log-slope varies considerably with horizontal position x. In order to compare aerial images using the log-slope, one must pick an x-value to use. An obvious choice is the mask edge. Thus, all subsequent reference to the slope of the log-aerial image will be at the mask edge. Now the effect of defocus on the aerial image can be expressed by plotting log-slope as a function of defocus, as shown in Figure 3. Superimposed on this curve is a graph of the ratio of center to edge intensities. It is very interesting to note that these two metrics of image quality give nearly identical variation with defocus to within a scale factor. Thus, the use of the log-slope is sufficient to characterize the degradation of the aerial image with defocus.

$\partial \ln I / \partial x \ (\mu m^{-1})$

0.6 μm lines and spaces
NA = 0.35
σ = 0.5
λ = 436 nm

no defocus

0.5 μm defocus

1.0 μm defocus

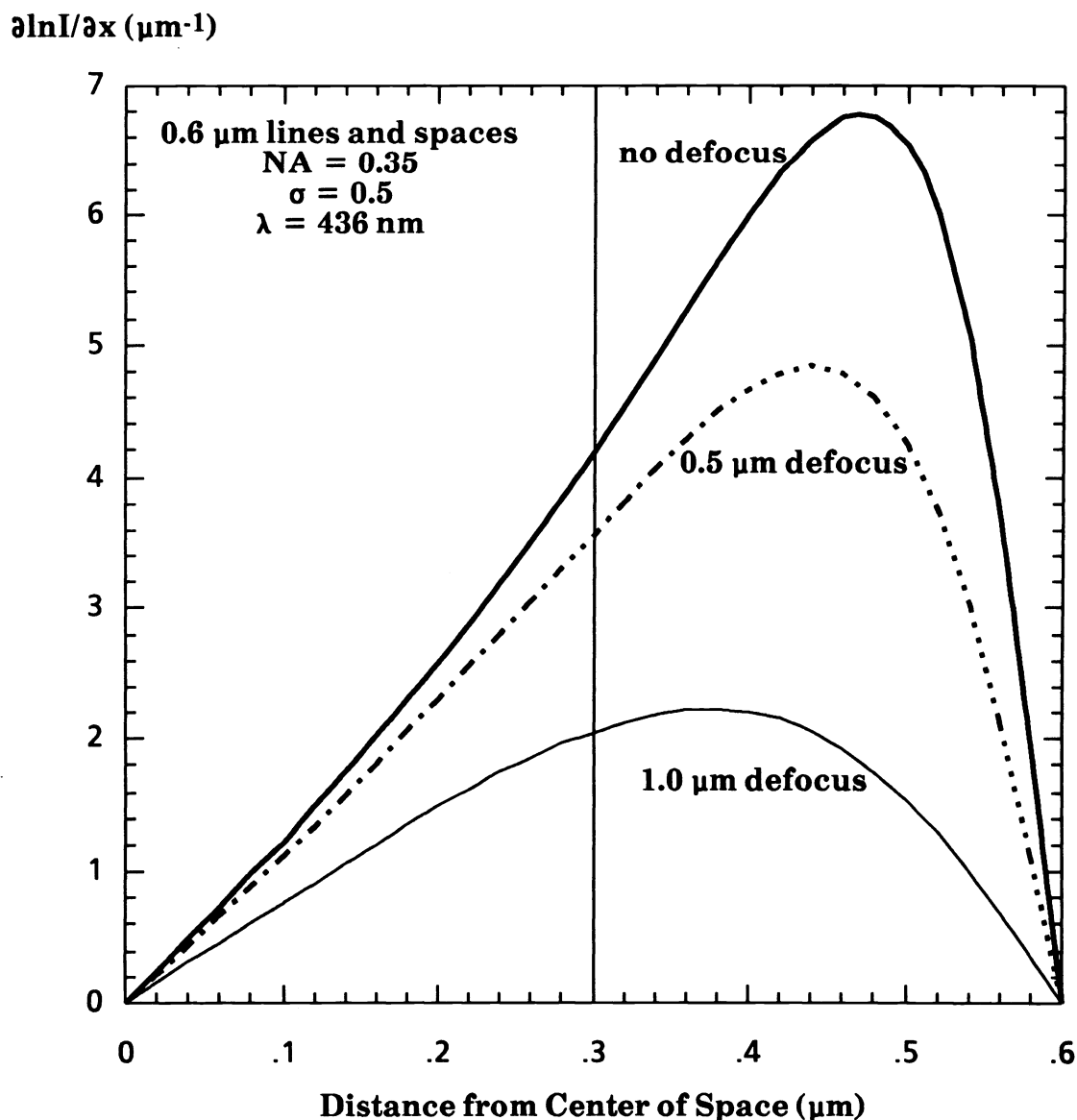Distance from Center of Space (μm)

Figure 2 : Variation of the slope of the log-image with horizontal position. The mask edge is represented by the vertical line.

Some very useful information can be obtained from a log-slope versus defocus curve. As was previously discussed, both process latitude and sidewall slope vary directly with the log-slope of the image. Thus, minimum acceptable process latitude and sidewall slope specifications translate directly into a minimum acceptable value of the log-slope. The log-slope versus defocus curve then can be used to give a maximum defocus to keep the process within this specification. If, for example, the minimum acceptable log-slope of a given process was determined to be 3.5 μm^{-1}, the maximum defocus of 0.6 μm lines and spaces on a 0.35 NA g-line printer would be, from Figure 3, about $\pm$ 0.5 μm. This gives a practical definition of the depth-of-focus that separates the effects of the aerial image and the photoresist process. The printer determines the shape of the log-slope defocus curve and the process determines the range of operation (i.e., the minimum log-slope). If the minimum log-slope was 4.5 μm^{-1}, one would conclude from Figure 3 that this printer could not adequately resolve 0.6 μm lines and spaces. Thus, resolution can also be determined from a log-slope defocus curve.
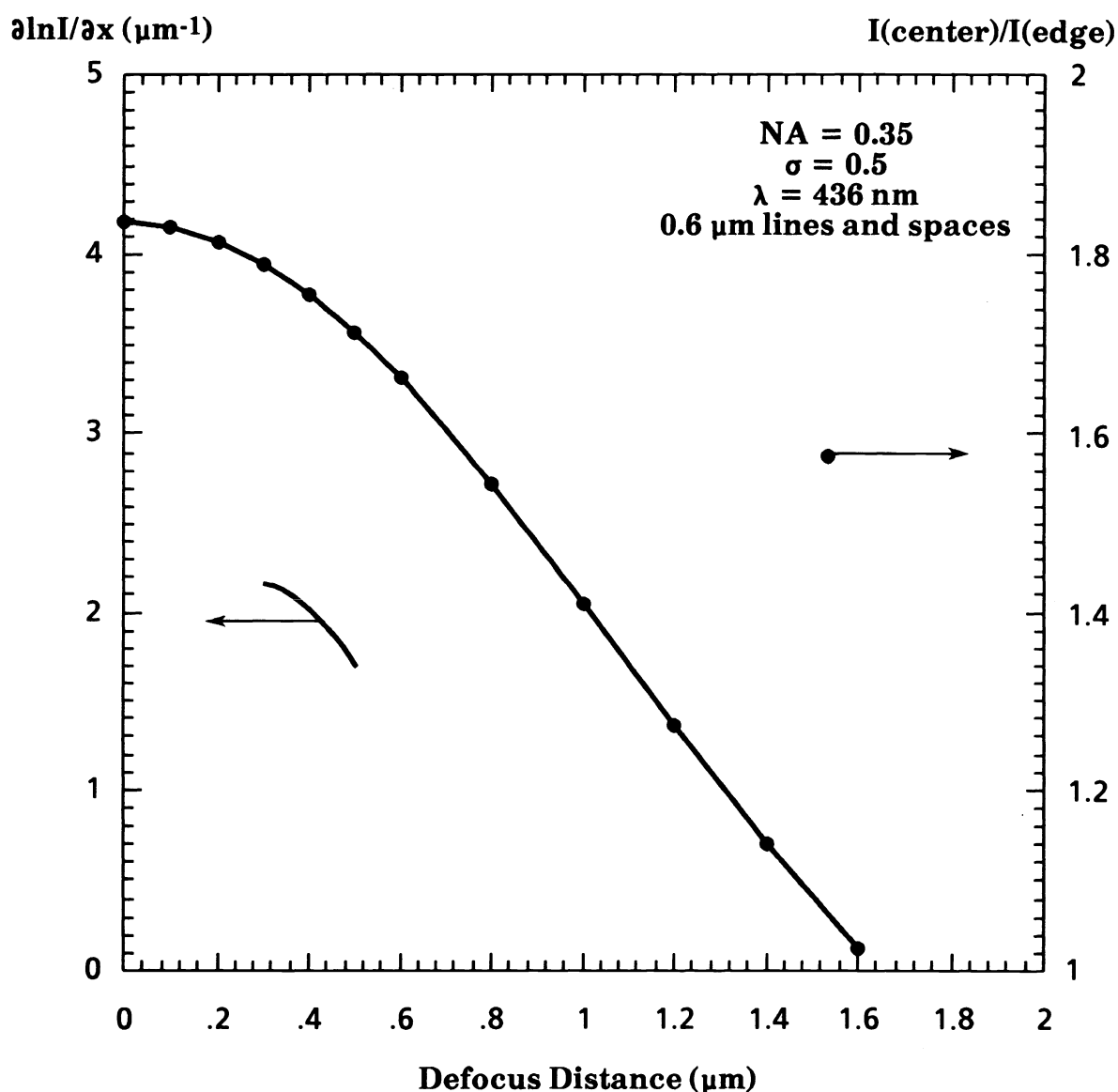

Figure 3 : Comparison of the two possible metrics of image quality.

Resolution can be defined in a manner similar to depth-of-focus. Consider Figure 4, which shows the effect of feature size on the log-slope defocus curve. If, for example, a log-slope of 3.5 μm^{-1} is required by a particular photoresist process, one can see that the 0.6 μm features will not be resolved, the 0.7 μm features will be resolved only when in perfect focus, the 0.8 μm features will have a DOF of ± 1 μm, and the 0.9 μm features will have a DOF of ± 2 μm. Obviously, the depth-of-focus is extremely sensitive to feature size, a fact which is not evident in the common Rayleigh definition. Since DOF is a strong function of feature size, it is logical that resolution is a function of depth-of-focus. Thus, in the situation shown in Figure 4, if the minimum acceptable DOF is ± 1 μm, the practical resolution is 0.8 μm lines and spaces. Resolution and depth-of-focus can not be independently defined.

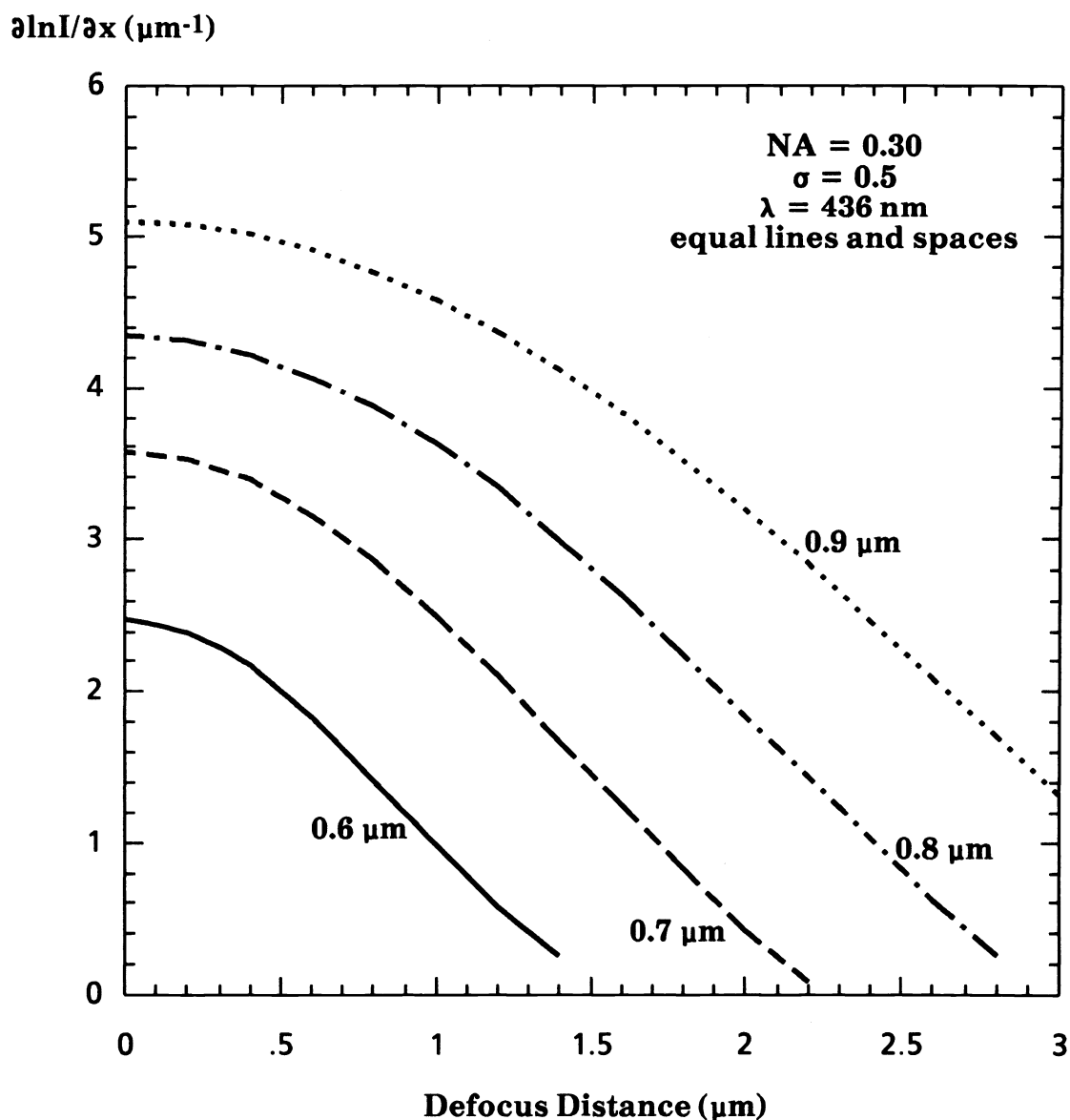$\partial \ln I / \partial x$ (μm^{-1})

Figure 4 : The effect of feature size and focus on the edge slope of the log-aerial image.
The resolution/depth-of-focus can be determined from these curves.

The log-slope defocus curve can now be used to explore the effects of various parameters on the resolution and depth-of-focus. The numerical aperture is one of the most important parameters defining lithographic performance and yet it is the most misunderstood. The Rayleigh DOF seems to predict a dramatic decrease of DOF with increasing numerical aperture. Shown in Figure 5 is the effect of numerical aperture on the log-slope defocus curve of 0.6 μm lines and spaces. The effect is to improve the aerial image log-slope for all values of defocus. Thus, the DOF increases with increasing numerical aperture for a given feature size. Note that as the log-slope goes to zero, all of the curves seem to converge to a single defocus value. Thus, in the limit of an infinite contrast photoresist process (i.e., one that resolves any feature with a log-slope greater than zero), numerical aperture does not affect resolution or depth-of-focus.

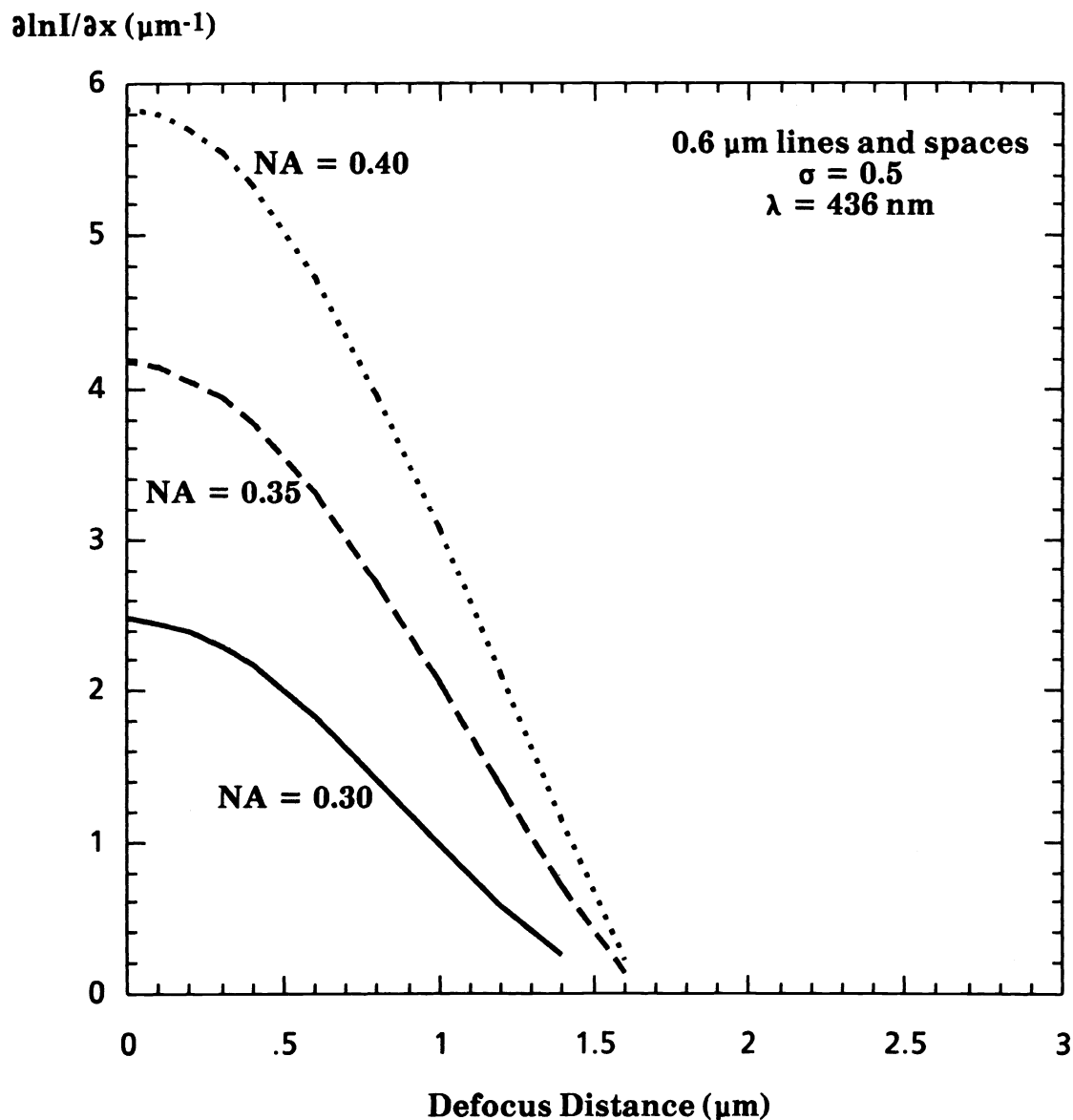$\partial lnI/\partial x \ (\mu m^{-1})$

Figure 5 : The effect of numerical aperture on focus latitude using the edge slope of the log-aerial image as a measure.

The role of wavelength in depth-of-focus is also misunderstood. Although equation (2) seems to indicate worse DOF with shorter wavelength, Figure 6 shows that DOF improves as wavelength decreases. Note that the effect of wavelength is different from numerical aperture in that the curves do not converge at zero slope. Rather, reducing wavelength improves DOF even as the log-slope goes to zero. Figures 5 and 6 show clearly the danger of using the Rayleigh criterion for comparing the DOF of different printers (i.e., different values of wavelength and numerical aperture).
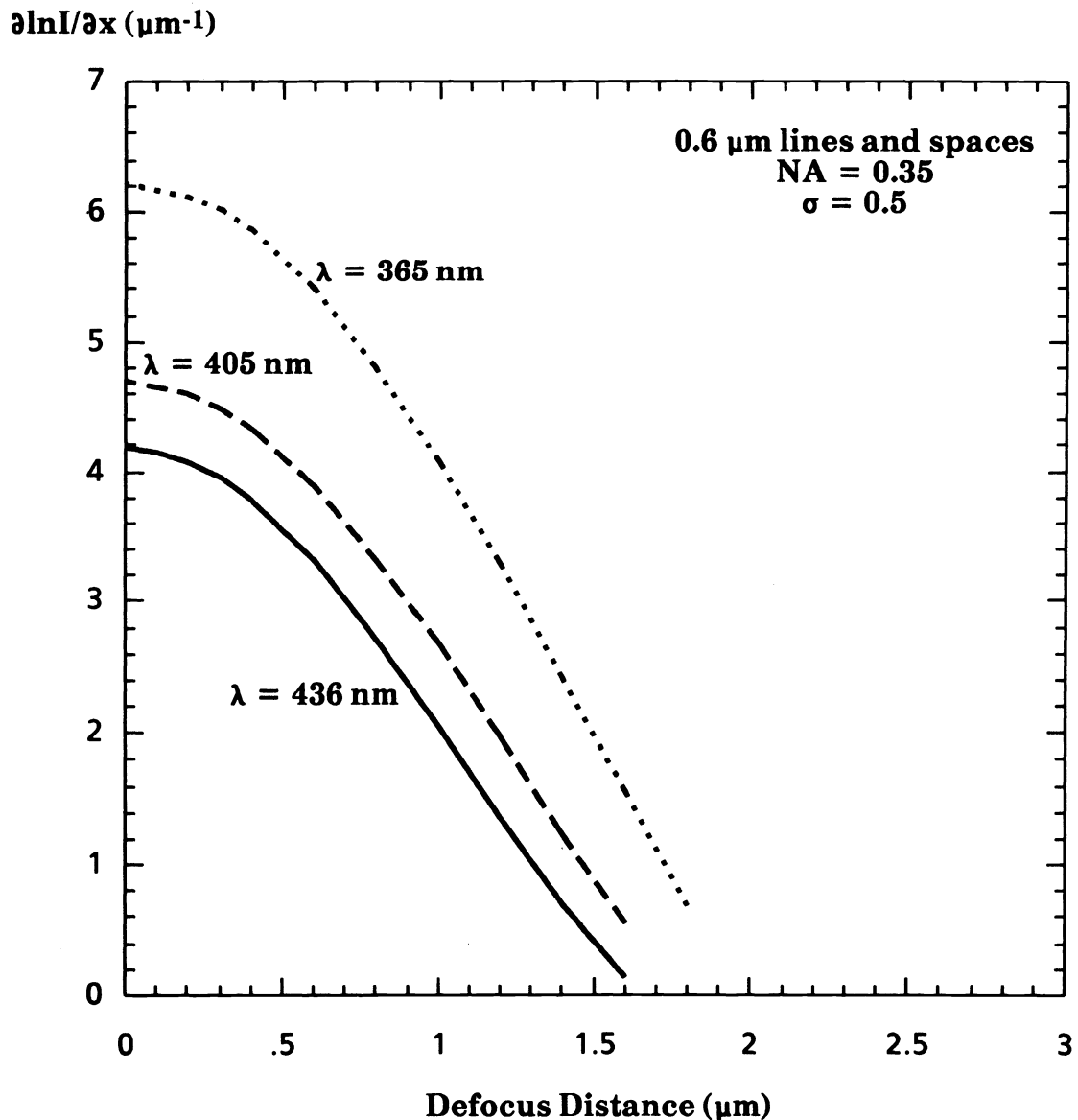
∂lnI/∂x (µm⁻¹)

Figure 6 : The effect of wavelength on focus latitude using the
edge slope of the log-aerial image as a measure.

The log-slope defocus curve can also be used to compare different printers in an objective manner. For example, there has been much discussion on the advantages of lower wavelength versus higher numerical aperture. It is common to compare a g-line, 0.42 NA system with an i-line, 0.35 NA machine. Both have the same value of λ/NA (almost) and thus, according to the Rayleigh criterion, the same resolution. In terms of the log-slope curve, the same value of λ/NA corresponds to the same value of the log-slope of the image with no defocus (Figure 7). The practical resolution is defined as the smallest feature which meets a given log-slope specification over a given focus range. If a process requires a log-slope of 4 μm^{-1} and a focus budget of ± 1 μm, Figure 7 shows that the i-line system will resolve a 0.6 μm feature, but the g-line system will not. Thus, the lower wavelength system has better resolution even though λ/NA is the same.
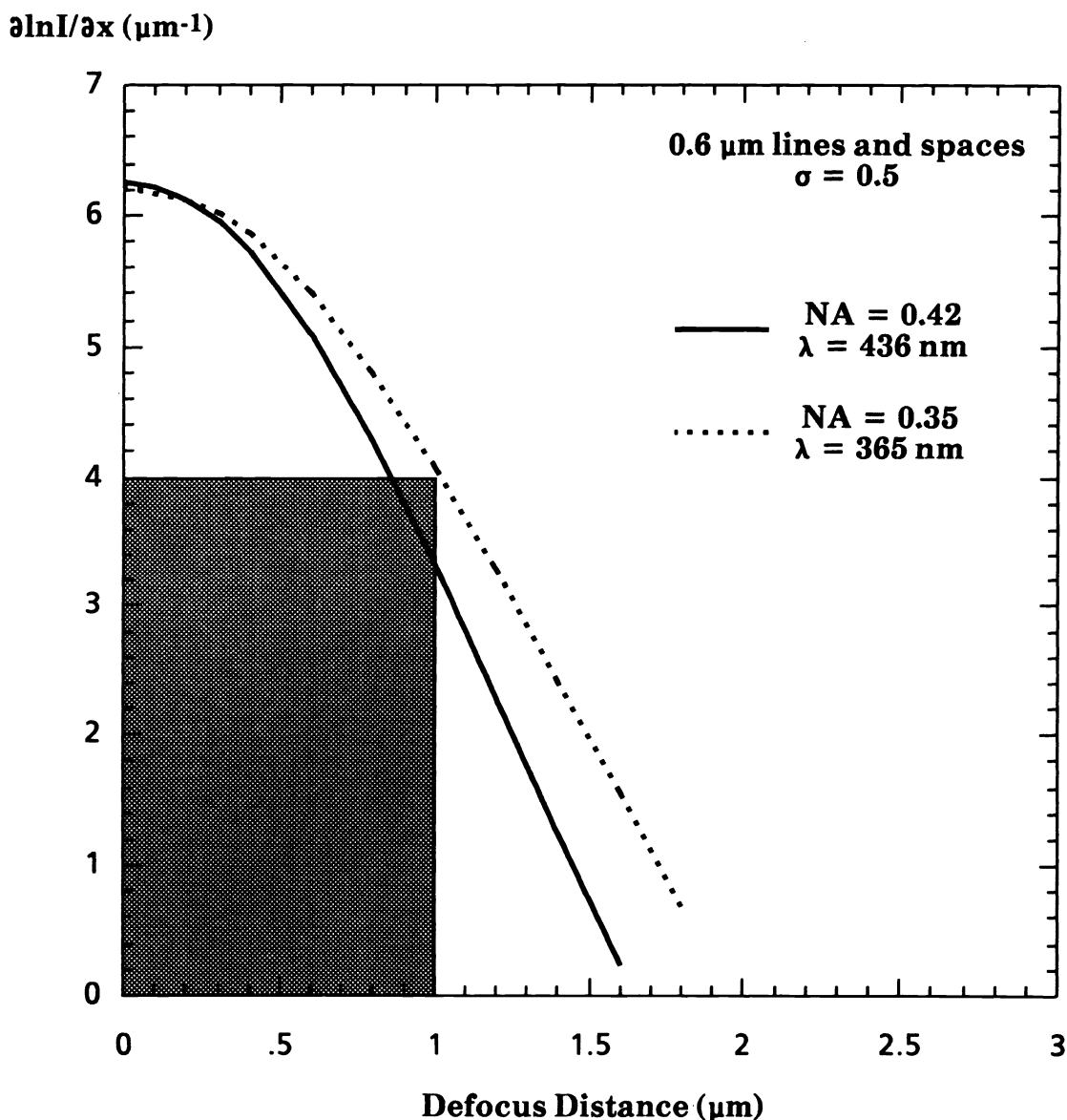
$\partial \ln I / \partial x$ (μm^{-1})

Figure 7 : Two printers with nominally the same resolution (i.e., the same λ/NA), in fact do not have the same practical resolution.

It is important to note that all of the aerial image calculations presented in this paper assume diffraction-limited lens performance, that is, ideal lenses. Obviously, the ideal lens does not exist and thus real lenses have log-slope versus defocus curves which are degraded to some extent. When comparing different lenses, as was done above, one must keep in mind that one lens may be further from the ideal than the other.

As a final example, Figure 8 shows the differences between an isolated line, an isolated space and equal lines and spaces. The differences are quite remarkable. As expected, packed lines and spaces have the worst resolution/depth-of-focus. Interestingly, the curves for isolated features cross, in this case at about 1 μm defocus. For defocus less than 1 μm the isolated line has better image quality than the space. But for greater defocus the isolated line falls off quite rapidly, and the isolated space has the better quality image.
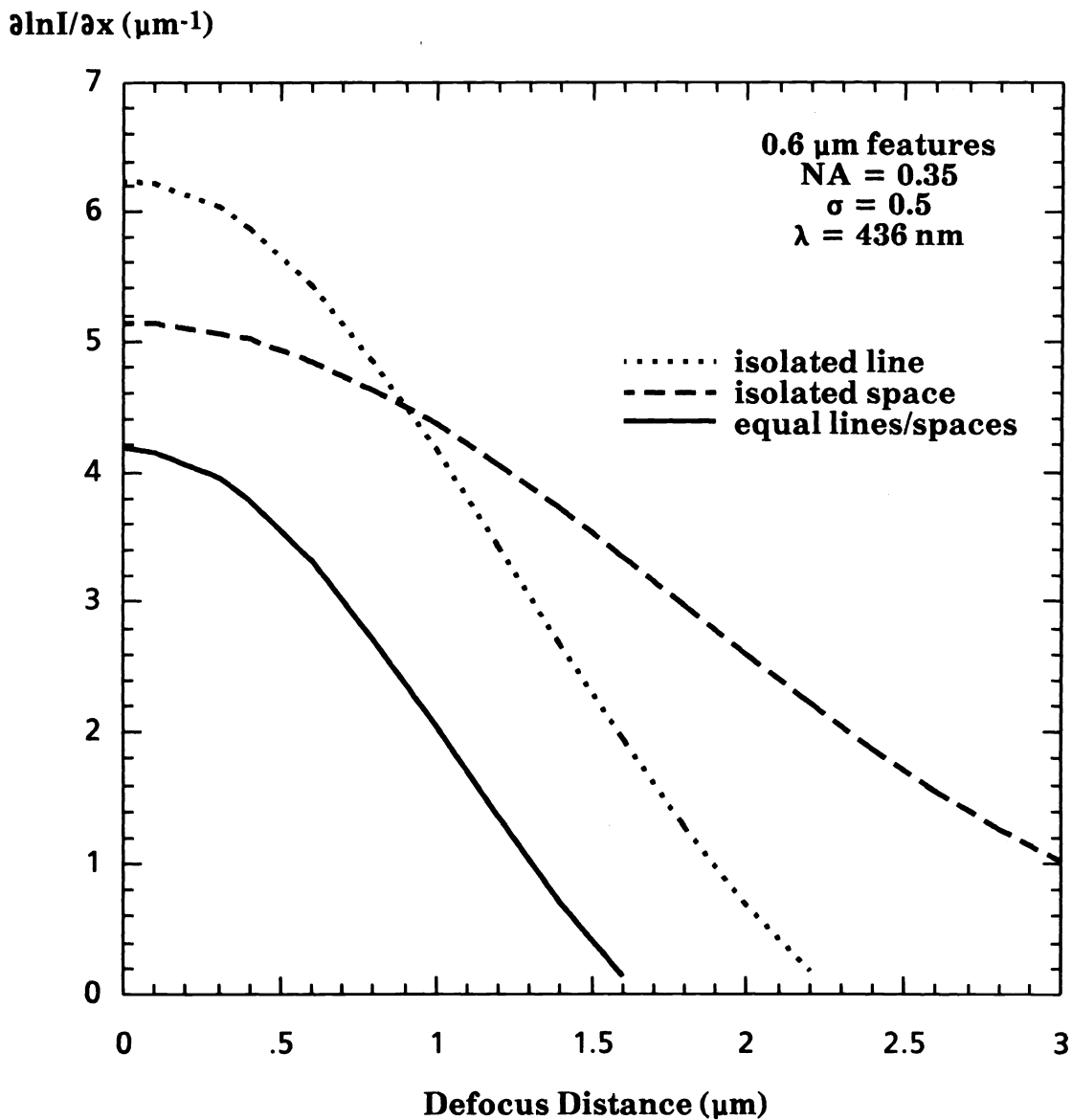
$\partial \ln I / \partial x$ (μm^{-1})

Figure 8 : The effect of feature type on focus latitude using the
edge slope of the log-aerial image as a measure.

3. PROLITH v1.4

Primary parameter lithography models such as PROLITH can be used to study the effects of focus on the lithographic process in detail. Previously, these models have all assumed that the aerial image is a constant throughout the thickness of the resist film. This is equivalent to saying that the resist thickness is less than the depth-of-focus of the process so that the image does not defocus as it propagates through the resist. In submicron imaging, however, this approximation is no longer valid. Thus, in order to accurately describe the effects of focus in submicron optical lithography one must take into account the defocusing within the resist. The most rigorous solution to this problem is to calculate the image in two or three dimensions using, for example, the extended source method of Yeung [7]. Such rigorous approaches are quite complicated, however, and a simple extension of current modeling techniques will now be proposed.

An integral part of current lithography models such as PROLITH is the assumption that the image is a plane wave traveling normal to the resist surface. In such a case the aerial image $I_i(x)$ and the standing wave intensity $I_s(z)$ may be calculated independently. The total intensity is

$$I(x,z) = I_i(x)I_s(z) . \tag{8}$$

where z is the depth into the resist and is zero at the top. The rigorous solution of Yeung does not make these assumptions and the total intensity is not separable. To avoid the complications of Yeung's calculations, we will assume that the aerial image and standing wave intensity are still separable, but make the aerial image a function of depth into the photoresist.

$$I(x,z) = I_i(x,z)I_s(z) . \tag{9}$$

The image $I_i(x,z)$ is calculated using the standard aerial image model by defocusing different amounts for different values of z. The depth into the resist is not the defocus distance, however. Rather, the defocus distance δ is given by [6]

$$\delta(z) = \delta_0 + z/n . \tag{10}$$

where δ_0 is the defocus distance at the top of the resist and n is the index of refraction of the resist. Although the aerial image is an even function of defocus (a defocus distance of $-\delta$ produces the same image as a defocus of δ), it is not an even function of δ_0. Since δ_0 can be thought of as the vertical position of the wafer plane in a stepper, focus effects in submicron lithography are not symmetric about the optimum focal position. In fact, defining the optimum focal plane becomes ambiguous when the resist thickness is not negligible compared to the DOF.

PROLITH v1.4 includes the defocus model described above. Using this program, the effects of defocus and exposure on submicron features can be simulated. Shown in Figure 9 are the common linewidth versus focus curves for different values of exposure. The defocus distance δ_0 is zero when the focal plane is at the top of the resist. If the wafer is moved upwards 1 μm from this position, the value of δ_0 is -1 μm. One can see that these curves are not symmetric. The optimum exposure appears to be about 120-125 mJ/cm^2 with mask bias, or about 100 mJ/cm^2 without. The optimum focal position is about -0.3 to -0.5 μm. In other words, the focal plane should be about 1/3 to 1/2 of the way down into the resist.

Another way to represent the data of Figure 9 is the focus-exposure process volume. In Figure 10, the values of focus and exposure which result in a ±10% variation in linewidth from the nominal are plotted. The result is a process window, within which the linewidth specification is met. Other specifications, such as sidewall angle, can also be plotted [6], as shown in Figure 10.
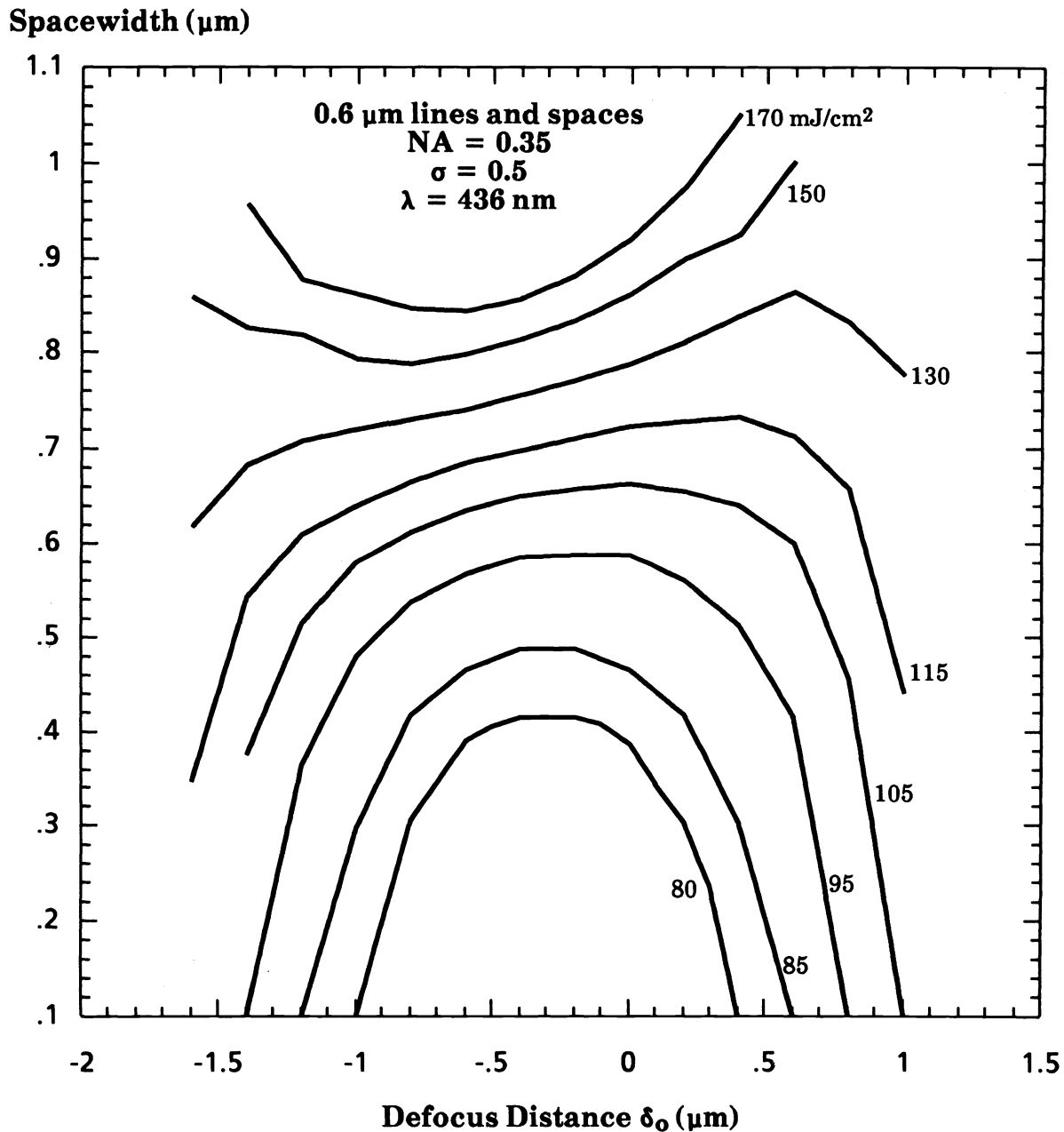
Spacewidth (µm)

Figure 9 : Focus latitude as a function of exposure as predicted by PROLITH.
A 1 µm resist with typical g-line parameters was assumed.

4. Conclusions

The Rayleigh criteria for resolution and depth-of-focus are not adequate in describing submicron optical lithography. In fact, it is quite easy to misinterpret the Rayleigh criteria and make completely inaccurate conclusions. Thus, a new approach to characterizing resolution and depth-of-focus has been introduced. By examining the interaction of the lithographic tool (via the aerial image) with the photoresist process, a metric for judging aerial image quality has been established. By examining the effects of feature size and defocus on this metric, accurate and meaningful definitions

of resolution and depth-of-focus can be made. This technique also leads to an understanding of the influence of various parameters on the depth-of-focus/resolution and the ability to compare the theoretical performance of different lithographic tools.

An enhanced version of PROLITH (the Positive Resist Optical Lithography model) has been introduced which accounts for defocus within the photoresist layer (in an approximate way). With this model, various focus effects can be characterized.
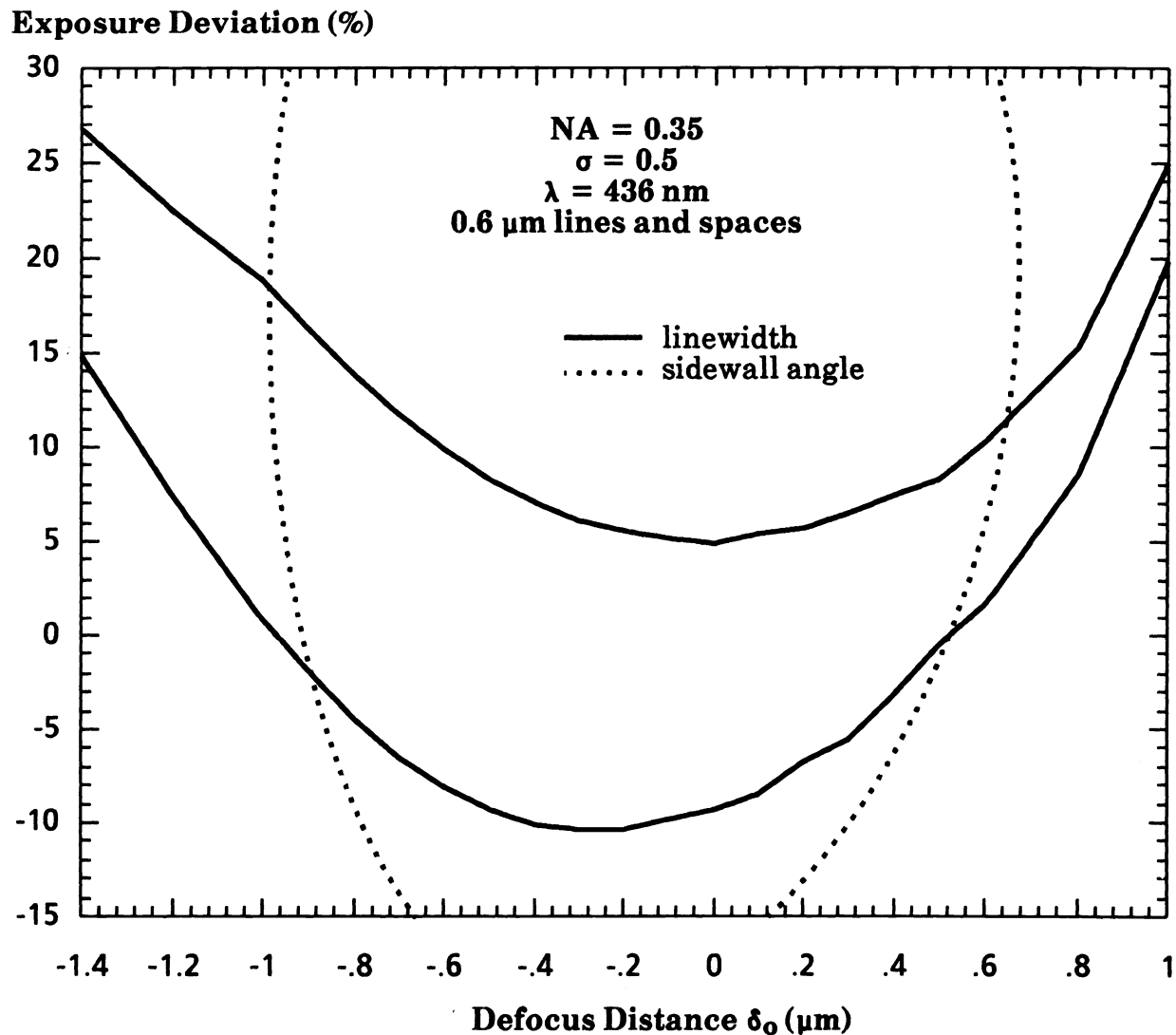
Exposure Deviation (%)

Defocus Distance δ_0 (μm)

Figure 10 : Focus-exposure process volume for ± 10% linewidth and 75 degree sidewall angle specifications (as predicted by PROLITH).

References

1. C. A. Mack, "Photoresist Process Optimization," *KTI Microelectronics Seminar Interface '87* (1987).

2. R. Hershel and C. A. Mack, "Lumped Parameter Model for Optical Lithography," Chapter 2, <u>Lithography for VLSI, VLSI Electronics - Microstructure Science</u>, R. K. Watts and N. G. Einspruch, eds., Academic Press (New York:1987) pp. 19-55.

3. C. A. Mack, "PROLITH: A Comprehensive Optical Lithography Model," *Optical Microlith. IV, Proc.*, SPIE Vol. 538 (1985) pp. 207-220.

4. C. A. Mack, "Advanced Topics in Lithography Modeling," *Adv. Resist Tech. III, Proc.*, SPIE Vol. 631 (1986) pp. 276-285.

5. H. J. Levinson and W. H. Arnold, "Focus: The Critical Parameter for Submicron Lithography," *Jour. Vac. Sci. Tech.*, Vol. B5, No. 1 (Jan/Feb 1987) pp. 293-298.

6. W. H. Arnold and H. J. Levinson, "Focus: The Critical Parameter for Submicron Optical Lithography: Part 2," *Optical Microlith. VI, Proc.*, SPIE Vol. 772 (1987) pp. 21-34.

7. M. Yeung, "Modeling Aerial Images in Two and Three Dimensions," *Kodak Microelectronics Seminar Interface '85* (1985) pp. 115-126.